Journal of Applied Physics

The structural and in-plane dielectric/ferroelectric properties of the epitaxial (Ba, Sr)(Zr, Ti)O_3 thin films

Cite as: J. Appl. Phys. **115**, 234102 (2014); https://doi.org/10.1063/1.4883963
Submitted: 20 April 2014 . Accepted: 05 June 2014 . Published Online: 16 June 2014

N. Y. Chan, D. Y. Wang, Y. Wang, J. Y. Dai, and H. L. W. Chan

View Online

Export Citation

CrossMark

ARTICLES YOU MAY BE INTERESTED IN

$BaTiO_3$-based piezoelectrics: Fundamentals, current status, and perspectives
Applied Physics Reviews **4**, 041305 (2017); https://doi.org/10.1063/1.4990046

Phase diagrams and dielectric response of epitaxial barium strontium titanate films: A theoretical analysis
Journal of Applied Physics **91**, 9288 (2002); https://doi.org/10.1063/1.1473675

Dielectric behavior of $Ba(Ti_{1-x}Zr_x)O_3$ single crystals
Journal of Applied Physics **88**, 410 (2000); https://doi.org/10.1063/1.373674

Lock-in Amplifiers
Find out more today

Zurich Instruments

© 2014 AIP Publishing LLC.

JOURNAL OF APPLIED PHYSICS 115, 234102 (2014)

The structural and in-plane dielectric/ferroelectric properties of the epitaxial (Ba, Sr)(Zr, Ti)O_3 thin films

N. Y. Chan,[1,a)] D. Y. Wang,[2] Y. Wang,[1] J. Y. Dai,[1,3] and H. L. W. Chan[1]
[1]*Department of Applied Physics, The Hong Kong Polytechnic University, Hung Hom, Kowloon, Hong Kong, China*
[2]*School of Materials Science and Engineering, The University of New South Wales, Sydney, New South Wales 2052, Australia*
[3]*Shenzhen Research Institute, The Hong Kong Polytechnic University, People's Republic of China*

(Received 20 April 2014; accepted 5 June 2014; published online 16 June 2014)

Epitaxial $(Ba_{1-x}Sr_x)(Zr_{0.1}Ti_{0.9})O_3$ (BSZT, $x = 0 - 0.45$) thin films were deposited on $(LaAlO_3)_{0.3}(Sr_2AlTaO_6)_{0.35}$ (LSAT) substrates by pulsed laser deposition. The experimental results demonstrate that the structural, dielectric, and ferroelectric properties of the BSZT thin films were greatly dependent on the strontium content. The BSZT thin films transformed from tetragonal to cubic phase when $x \geq 0.35$ at room temperature. The Curie temperature and room-temperature remnant polarization decrease with increasing strontium concentration. The optimal dielectric properties were found in $(Ba_{0.55}Sr_{0.45})(Zr_{0.1}Ti_{0.9})O_3$ thin films which is in paraelectric state, having tunability of 47% and loss tangent of 0.0338 under an electric field of 20 MV/m at 1 MHz. This suggests that BSZT thin film is a promising candidate for tunable microwave device applications. *© 2014 AIP Publishing LLC*. [http://dx.doi.org/10.1063/1.4883963]

I. INTRODUCTION

Perovskite-structured ferroelectric thin films have attracted extensive attention in recent years due to their unique properties such as large spontaneous polarization, high dielectric constant, large dielectric tunability, and low dielectric loss. Such a variety has led to suitable for complex oxide based microelectronics applications, such as microwave phase shifters, tunable filters, high Q resonators for radar, and communication.[1–3]

Among many material families, (Ba,Sr)TiO_3 (BST) is one of the promising candidates for tunable microwave applications. In BST, the increase of Sr concentration can lead to the lowering of the Curie temperature with a rate of ~3.8 °C per molar % of Sr (Refs. 4 and 5) and the Curie temperature of BST can be tailored over a board composition range in order to meet the specific requirements of device design. Another possible way to tune the Curie temperature of the $BaTiO_3$ system is to substitute Ti by Zr. As Zr^{4+} (0.087 nm) is more chemically stable than Ti^{4+} (0.068 nm), the addition of Zr in BST can also improve the chemical stability and reduce the dielectric loss.[6,7] The substitution of Ti with Zr would depress the conduction by electronic hopping between Ti^{4+} and Ti^{3+} ion which maintains a low leakage current. The structural, dielectric, and ferroelectric properties of Ba(Zr, Ti)O_3 (BZT) ceramics, showing strong dependence on the Zr content, have been reported in the literatures.[8–10]

The simultaneous addition of Zr and Sr into $BaTiO_3$ will result in (Ba,Sr)(Zr,Ti)O_3 (BSZT) system.[4,5,11–13] Compared with conventional BST and BZT thin films, (Ba,Sr)(Zr,Ti)O_3 materials have dopant on both the Ba-sites and Ti-sites, which may offer a better structural modifiability and hence more flexibility for property optimizations. The Zr/Ti ratio is very important in BZT system. For Zr content less than 10 at. %, the material shows normal ferroelectric behavior.[14,15] As the Zr content increases up to 20 at. %, the BZT system shows diffuse phase transition at Curie temperature, further increasing Zr content results in relaxor behavior. For typical ABO_3 perovskite, the physical properties can be altered by site engineering on A or/and B sites through substitution, the discovery of high performance $Ba(Zr_{0.2}Ti_{0.8})O_3$-x $(Ba_{0.7}Ca_{0.3})TiO_3$ system, with giant piezoelectric coefficient at around MPB composition $(Ba_{0.85}Ca_{0.15})(Zr_{0.1}Ti_{0.9})O_3$ stimulated an extensive research in the field of co-substituted $BaTiO_3$ family material as promising alternative to Pb(Zr,Ti)O_3 (PZT) system.[16–20] Simultaneous addition of Sr and Zr into the $BaTiO_3$ system is a feasible strategy of study because of the similar structure. However, the majority of existing studies on BSZT thin films were focused on the out-of-plane characterization based on metal-insulator-metal configurations at low frequency. The dielectric characteristics of the BSZT thin films along in-plane directions remain largely unknown. The in-plane configuration is more directly relevant to the actual coplanar devices. The capability to grow high performance thin films on single crystal substrates is one of the prerequisites for development of micro-system device.[21] In this paper, we present a systematic study of the Sr concentration effect on the structural, in-plane dielectric and ferroelectric properties of the epitaxial $(Ba_{1-x},Sr_x)(Zr_{0.1}Ti_{0.9})O_3$ (BSZT) thin films on $(LaAlO_3)_{0.3}(Sr_2AlTaO_6)_{0.35}$ (001) (LSAT) substrate. Based on the room-temperature phase diagram of the $(Ba_{1-x},Sr_x)(Zr_{0.1}Ti_{0.9})O_3$ system, a particular composition range x = 0–0.45 was chosen in this study to cover both ferroelectric and paraelectric phases.

II. EXPERIMENTAL DETAILS

KrF excimer laser with a wavelength of 248 nm and pulse duration of 25 ns (Lambda Physik COMPex 205) was

[a)]Author to whom correspondence should be addressed. Electronic mail: ngaiyuichan@gmail.com.

 © 2014 AIP Publishing LLC

used for the thin film deposition. The laser pulse repetition rate was fixed at 10 Hz with laser energy around 250mJ (energy density of 2–3 J/cm^2 on the target surface). The $(LaAlO_3)_{0.3}(Sr_2AlTaO_6)_{0.35}$ (LSAT) substrate was kept at 700 °C during the thin film deposition and thicknesses of the BSZT thin films are around 300 nm. The X-ray diffraction measurements were carried out using Bruker AXD D8 Discover X-ray diffractometer. The surface morphology of the thin films was studied using a Digital Instrument Nanoscope IV atomic force microscope (AFM) operating under tapping mode. Top Au electrodes were deposited by DC magnetron sputtering and followed by patterning using photolithography process. The electrical properties of the thin film were characterized based on interdigital capacitor (IDC) configuration (total 21 fingers with finger length of 925 μm, finger width of 5 μm, and finger gap spacing 2 μm). The fingers of the IDC were aligned along the in-plane $\langle 010 \rangle$ or $\langle 100 \rangle$ crystallographic directions. The IDC was wire bonded to a piece of PCB for easy handling and better electrical contact during subsequent measurements. To extract the dielectric properties of the thin film from the IDC, a MATHMATICSA program was developed based on the Gevorgian's model using the conformal mapping technique and the relative permittivity were calculated by a set of mathematical formulas.[22,23] The room-temperature relative permittivity of the BSZT thin films as a function of electric field and frequency was measured using an HP4294A impedance analyzer (measured frequency: 1 kHz–1 MHz) and an HP4291B RF impedance analyzer (measured frequency: 1 MHz–100 MHz). Ferroelectric property measurements were conducted by TF Analyzer 2000 equipped with a FE-Modulue (aixACCT, German) at 1 kHz.

III. RESULTS AND DISCUSSION

A. XRD and surface morphology

Figures 1(a)–1(f) show the θ-2θ spectra of (001) oriented BSZT thin films deposited on the LSAT (001) substrates. All the films exhibited single phase perovskite structure with no detectable impurity or other phases. The full width at half maximum (FWHM) of the rocking curves (ω-scan) for BSZT (002) reflections are shown in the insets. The grain orientation is known to be a key factor which determines the quality of the thin films. The FWHM values of the BSZT thin films are below 0.25°, indicating the grains are uniformly aligned in all the films. The off axis φ-scans of (202) diffraction peak as shown in Figure 1(g) were performed to understand the in-plane growth relationship between the film and the substrate. The four-fold symmetric (202) diffraction peaks of the films are very sharp and coincide well with those of LSAT (001) substrates, suggesting a cube-on-cube epitaxial growth relationship between the films and substrates with in-plane orientation relationship of $\langle 100 \rangle_{BSZT} // \langle 100 \rangle_{LSAT}$.

The evolutions of BSZT (002) and (202) peaks with increasing Sr content are shown in Figs. 2(a) and 2(b),

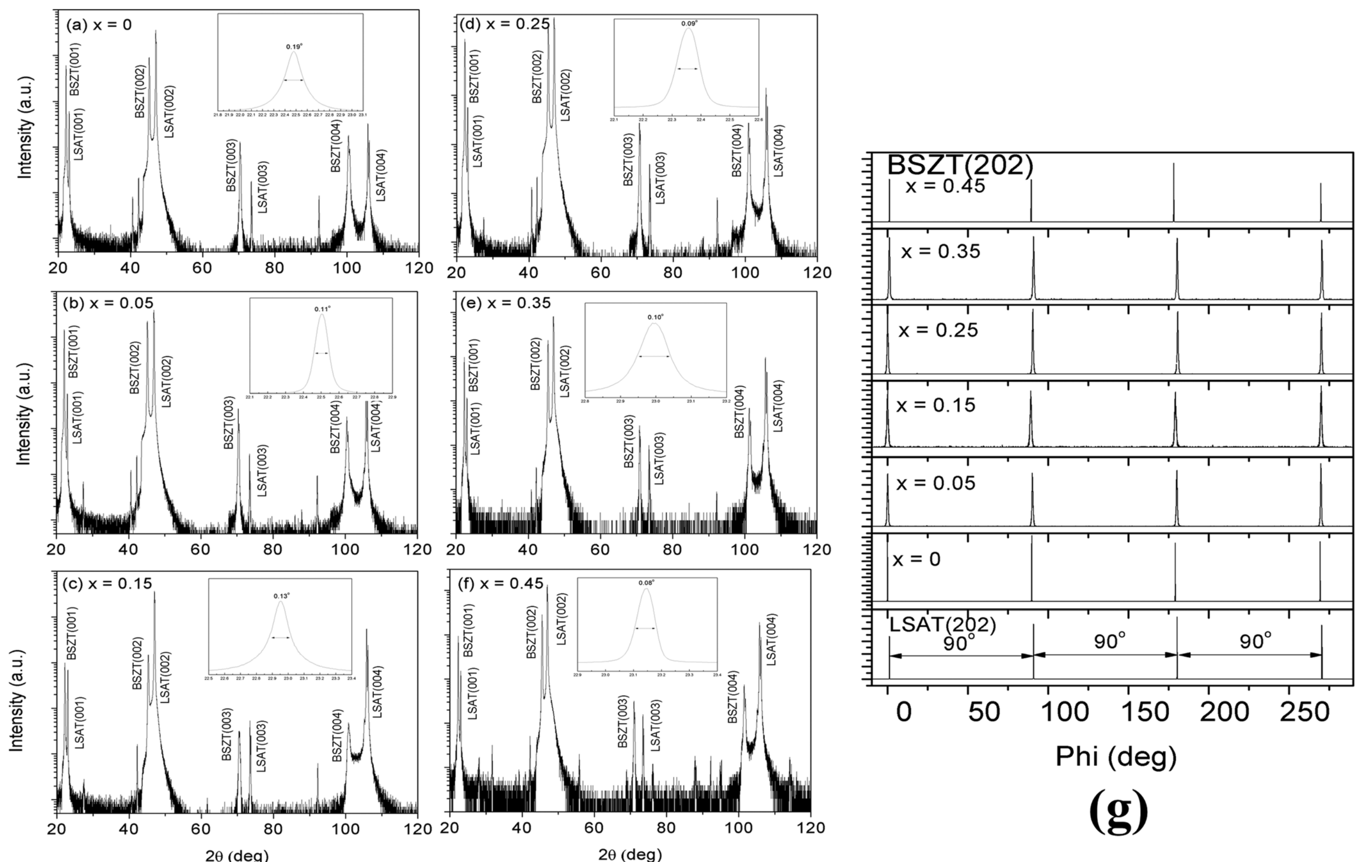

FIG. 1. (a)–(f) XRD θ-2θ scan pattern of $(Ba_{1-x},Sr_x)(Zr_{0.1},Ti_{0.9})O_3$ thin film grown on LSAT(001). (a) x = 0, (b) x = 0.05, (c) x = 0.15, (d) x = 0.25, (e) x = 0.35, (f) x = 0.45 (inset: ω- scan of the thin films); (g) Off axis φ scan of the (202) diffraction of BSZT thin films deposited LSAT(001) substrates.

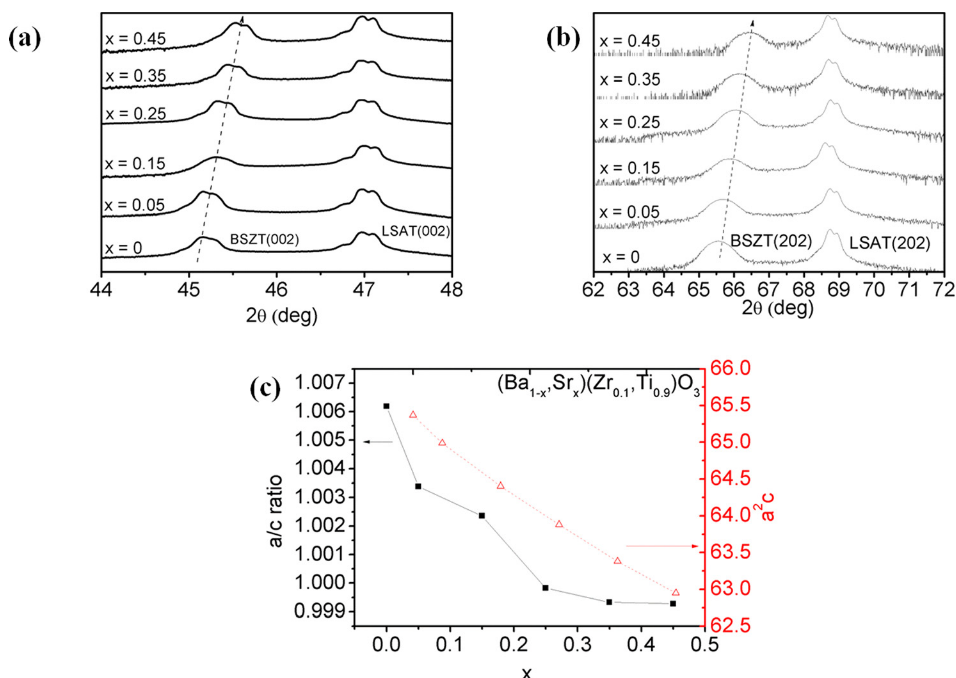

FIG. 2. (a) XRD θ-2θ scan patterns of $(Ba_{1-x},Sr_x)(Zr_{0.1},Ti_{0.9})O_3$ thin film grown on LSAT(001) substrates; (b) XRD θ-2θ scan pattern of $(Ba_{1-x},Sr_x)(Zr_{0.1},Ti_{0.9})O_3$ thin film grown on LSAT(001) substrates with $\chi = 45°$. (c) Tetragonality a/c and unit cell volume a^2c of BSZT thin films deposited on LSAT(001) substrates as a function of Sr content.

respectively. With the increase in Sr content, both (002) and (202) peaks of BSZT shift to higher angles, implying the contraction of unit cells. The out-of-plane and in-plane lattice parameters decrease with the increase in Sr content since the ionic radius of Ba^{2+} (1.61 Å) is larger than that of Sr^{2+} (1.44 Å). More Sr^{2+} substitution results in the decrease in lattice parameters. As shown in Figure 2(c), all the thin films show tetragonally distorted lattice structure, which is different from that calculated from their bulk counterparts,[24] indicating that structure of the thin films has been modified by the substrates. The deviations of lattice structure have also been reported in other perovskite thin films grown on single crystal substrates.[25–27] These deviations are probably induced by the strain generated from the lattice misfit and the thermal expansion mismatch between the film and the substrate as well as the presence of oxygen vacancies in the thin film. Figure 3 shows the surface morphology of the thin films, which exhibits strong dependence on the Sr concentration. The grain size of the thin films decreases with the increase in Sr content. On the other hand, a smooth surface with no microcracks and pinholes and a dense morphology were observed in all the BSZT thin film.

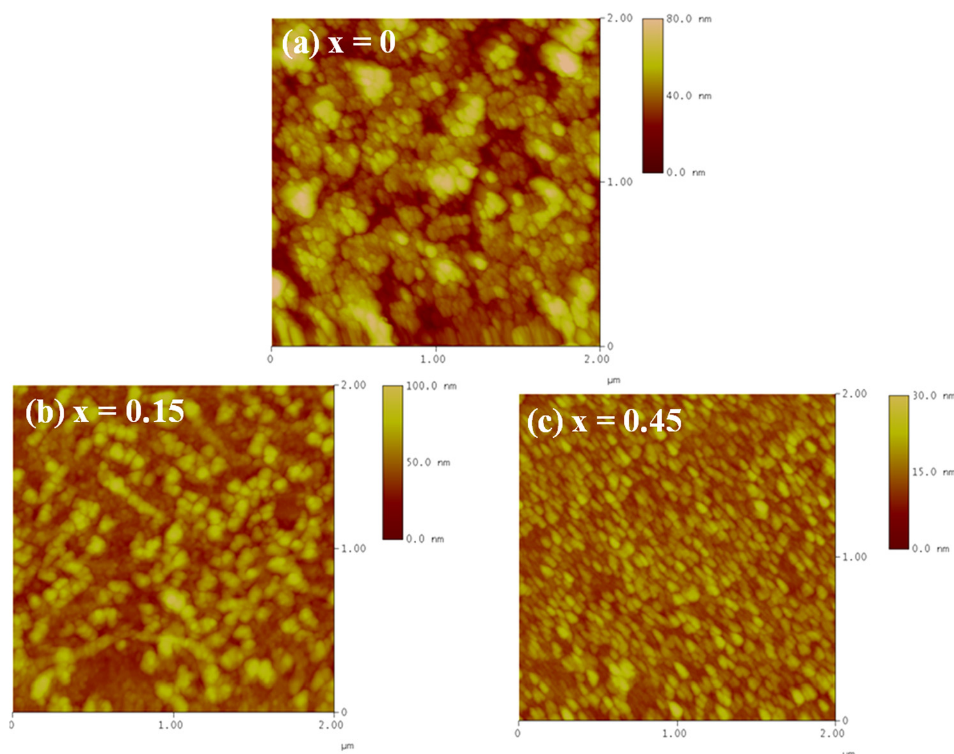

FIG. 3. Surface morphology of BSZT thin film deposited on LSAT (001) single crystal substrate. (a) x = 0, (b) x = 0.15, (c) x = 0.45.

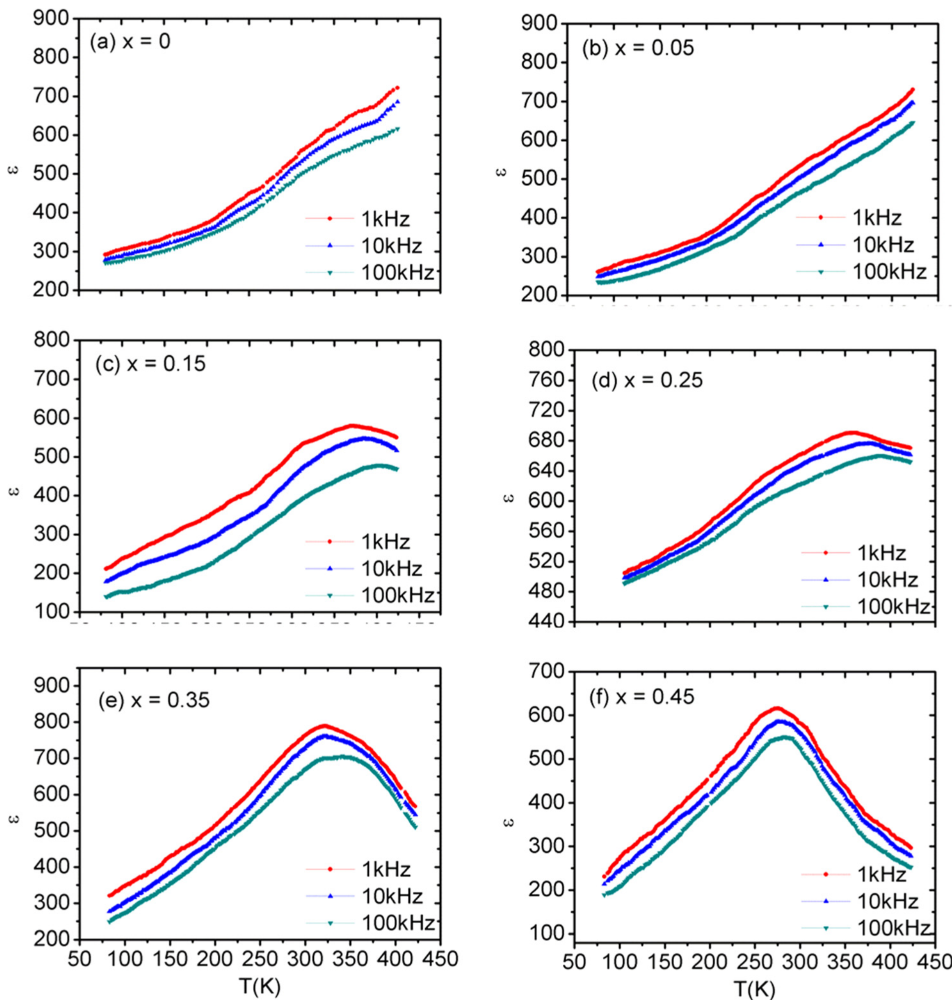

FIG. 4. Temperature dependence of the relative permittivity of BSZT thin films on LSAT measured using IDC.

B. Phase transition temperature and permittivity as a function of frequency

Figure 4 shows the temperature dependence of the relative permittivity ε of the BSZT thin films measured using IDC. As shown in the figure, the Curie temperature decreases with the increase of Sr content. It should be noted that the Curie temperatures of the thin films are higher than those of their bulk counterparts as listed in Table I. The relative permittivity of $Ba(Zr_{0.1}Ti_{0.9})O_3$ and $(Ba_{0.95}Sr_{0.05})(Zr_{0.1}Ti_{0.9})O_3$ thin films increase monotonically in the measuring temperature range and didn't exhibit any obvious phase transitions, implying their Curie points may be higher than the measuring range. Due to our instrumentation limit, the maximum measuring temperature is restricted to 150 °C. Frequency dispersion phenomena have been observed in the ε-T curves. It is noted that the phase transition peaks are much broader than those of the BSZT bulk ceramics. The broadening of the transition peaks in the films is presumably attributed to the small grain size. Such phenomenon has also been observed in other nano-grained ferroelectric $BaTiO_3$ thin films.[28] The upward shift of T_c can be attributed to in-plane lattice elongation as confirmed by XRD measurements, which is analogous to that reported in the literature.[29,30] In general, if there is a tensile stress along the in-plane direction, then the Curie temperature of the thin films measured along this specific direction is likely to shift toward higher temperature. Conversely, a compressive stress may lower the Curie temperature of the films. It has been reported that a biaxial tensile strain of order of 1% in ferroelectric thin films is enough to push the Curie temperature to a value much higher than its inherent value.[31,32] However, the upshift of T_c in our tensile-strained BSZT thin film is not significant as expected because the film thickness has exceeded its critical values, resulting in a relaxation towards a zero-strain state by the introduction of dislocations in the films. The large lattice misfit energy at the interface can only be released by creating lots of edge dislocations at the interface between the BSZT film and the substrate.[25,26] In addition, the relative permittivity of the BSZT thin films is lower than that of BSZT bulks and the degradation of the relative permittivity can be attributed to the reduction of crystallite size due to incorporation of Sr in the BZT lattice.

TABLE I. Transition temperature of $(Ba_{1-x}Sr_x)(Zr_{0.1}Ti_{0.9})O_3$ (x = 0, 0.05, 0.15, 0.25, 0.35, 0.45) thin films and bulk ceramics measured at 1 kHz.

	x = 0	x = 0.05	x = 0.15	x = 0.25	x = 0.35	x = 0.45
Bulk (°C)	97	88	62	39	8	−6
Thin film (°C)			97	80	23	10

Figure 5 shows relative permittivity of the BSZT thin films as a function of frequency. For $(Ba_{0.75}Sr_{0.25})(Zr_{0.1}Ti_{0.9})O_3$ thin

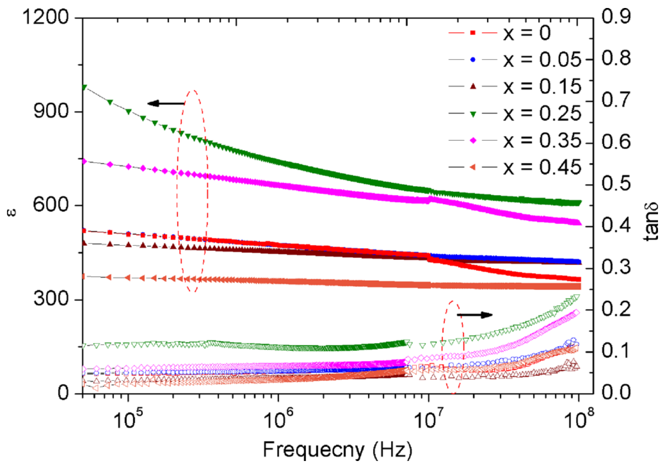

FIG. 5. Frequency dependence of the relative permittivity ε and loss tangent of $(Ba_{1-x},Sr_x)(Zr_{0.1},Ti_{0.9})O_3$ (x = 0, 0.05, 0.15, 0.25, 0.35, 0.45) thin films.

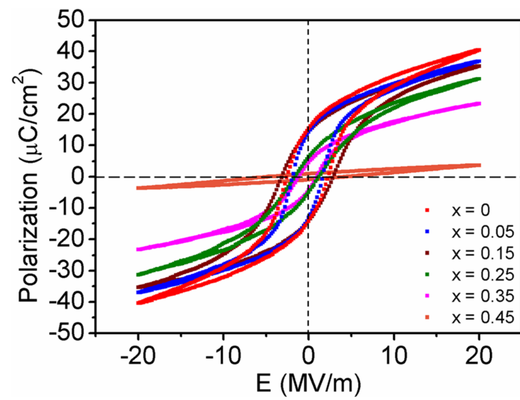

FIG. 6. Hysteresis loops of $(Ba_{1-x},Sr_x)(Zr_{0.1},Ti_{0.9})O_3$ (x = 0, 0.05, 0.15, 0.25, 0.35, 0.45) thin films.

film, the Curie transition temperature is close to room temperature and it shows highest relative permittivity and dielectric loss. At higher frequency, the dielectric loss of the thin film rises rapidly, which probably due to parasitic capacitance were not accounted for the circuit model of device under test. The dispersion can be strongly linked to the microstructure of the film and the low frequency dielectric dispersion in ferroelectric films can arise due to domain wall fluctuations, hopping conduction or space charge dispersion. As the frequency increases, parameters like wires, ferroelectric domains in thin film and electrodes influenced the dielectric dispersion at high frequency.

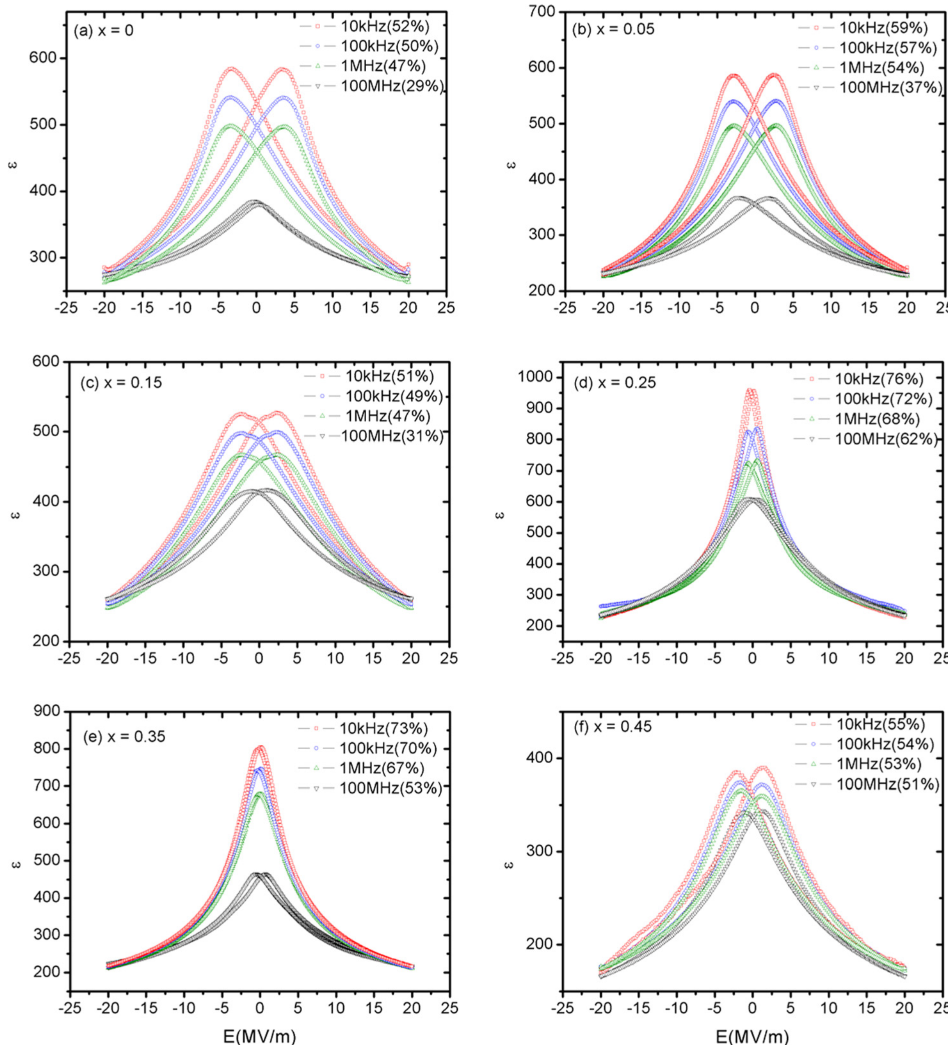

FIG. 7. Relative permittivity as a function of electric field for $(Ba_{1-x},Sr_x)(Zr_{0.1},Ti_{0.9})O_3$ (x = 0, 0.05, 0.15, 0.25, 0.35, 0.45) grown on LSAT.

C. Hysteresis loops

The ferroelectric properties of the BSZT thin films were evaluated by the electric polarization with applied electric field (P-E) hysteresis loop as shown in Figure 6. It is observed that the saturation remanent polarization P_r decreases with increasing Sr content in the films. The decrease in P_r can be attributed to two reasons: (1) smaller grain size in Sr modified BZT thin film inhibited the formation of large ferroelectric domains, which reduced the effective contribution to total polarization. (2) With the increasing Sr content, the Curie temperature of thin films decreases, leading to paraelectric behavior at room temperature. Thus, the polarization becomes weaker. The remnant polarization was well retained up to 15 $\mu C/cm^2$ for x = 0, but it degraded close to zero for x = 0.45. In $(Ba_{0.55}Sr_{0.45})(Zr_{0.1}Ti_{0.9})O_3$ thin film, the Curie temperature is below room temperature, and hence a slim P-E loop arises due to its paraelectric nature.

D. Dielectric tunability

Figure 7 shows the DC electric field (E) dependence of the relative permittivity (ε) of the BSZT thin films measured at room temperature. The ε – E characteristics of the BSZT thin films were determined over a number of selected frequencies (10 k, 100 k, 1 M, and 100 MHz). A strong dependence of the relative permittivity on the applied E-field was found. The typical butterfly shape of the ε-E curves is consistent with the room temperature ferroelectric state as observed from the ε-T and P-E measurements. Furthermore, with the increasing in the electric field, the relative permittivity as well as dielectric loss decreases. Such decrease in dielectric loss with increasing electric field is related to the pinning effect of domain or movable charge defects. The characterization of relative permittivity depending on the bias DC voltage provides a useful foreground in tunable devices. High tunability near the transition temperature is expected. For typical planar capacitor structure, the total capacitance is composed of three components: air, thin film, and substrate. In this configuration, tunability only comes from BSZT thin film since the LSAT substrate show no observable tunability in such small electric field. Figure 8 shows the frequency dependence of the dielectric tunability

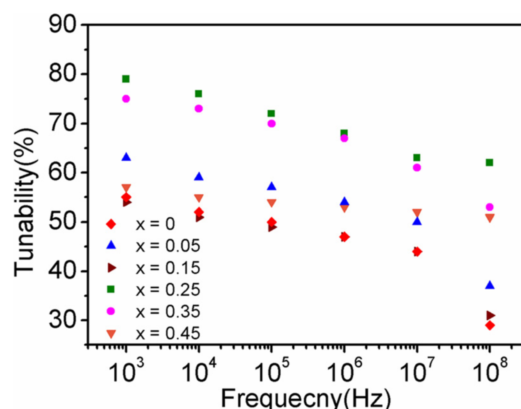

FIG. 8. The frequency dependence of dielectric tunability K(%) of the BSZT thin films under 20 MV/m.

TABLE II. Tunability, loss tangent and figure of merit for $(Ba_{1-x}Sr_x)(Zr_{0.1}Ti_{0.9})O_3$ (x = 0, 0.05, 0.15, 0.25, 0.35, 0.45) grown on LSAT.

	x = 0	x = 0.05	x = 0.15	x = 0.25	x = 0.35	x = 0.45
K at 1 MHz(%)	47	57	47	68	67	47
Loss at 1 MHz	0.0533	0.0531	0.0445	0.1043	0.0690	0.0338
FOM	8.81	10.7	10.6	6.5	9.7	13.9

K of $(Ba_{1-x},Sr_x)(Zr_{0.1},Ti_{0.9})O_3$ (x = 0 – 0.45) thin films under 20 MV/m biased field. In comparison to the parallel-plate capacitors, coplanar designs generally require higher driving voltage and offer lower tunability, but our results are comparable with some of the reported data on BSZT films based on parallel plate capacitors.[33–35] The relative permittivity of x = 0.25 is the largest compared with other thin films as its Curie temperature is close to room temperature. However, for practical applications, it is expected that material should not only have high tunability but also possess low dielectric loss. In this sense, paraelectric phase is more suitable for tunable device application than ferroelectric phase because the ferroelectric phase BSZT exhibits polarization hysteresis loop which significantly increases dielectric loss. Therefore, the figure of merit (FOM), which defined as $FOM = K(\%)/tan\delta$, is commonly used to characterize the overall performance of the dielectric materials. Maximum FOM up to ∼13.9 has been observed for $(Ba_{0.55}Sr_{0.45})(Zr_{0.1}Ti_{0.9})O_3$ thin film in paraelectric phase and the FOM of the thin film with different composition are listed in Table II.

IV. CONCLUSIONS

The compositional dependence of the structural and in-plane dielectric/ferroelectric properties of the $(Ba_{1-x}Sr_x)(Zr_{0.1}Ti_{0.9})O_3$ (x = 0 – 0.45) thin films grown on LSAT (001) single crystal substrates were studied. The dielectric and ferroelectric measurement were performed with the interdigital capacitor. It is revealed the ferroelectric state of the thin films is closely correlated with their in-plane tensile strain, i.e., upward shift of Curie temperatures as compared with their bulk counterpart. The optimal dielectric properties are found in $(Ba_{0.55}Sr_{0.45})(Zr_{0.1}Ti_{0.9})O_3$ thin film with a high tunability of 47%, low dielectric loss of 0.0338 at 1 MHz with a figure of merit ∼13.9. The low dielectric loss in $(Ba_{0.55}Sr_{0.45})(Zr_{0.1}Ti_{0.9})O_3$ thin film is attributed to its paraelectric nature at room temperature. Our results suggest that BSZT thin film is a promising candidate for tunable microwave application.

ACKNOWLEDGMENTS

N. Y. Chan would like to thank for the support of the Hong Kong Ph.D. Fellow Scheme from the Research Grants Council of Hong Kong No. RUY3. Jiyan Dai acknowledges the support from the National key Basic Research Program of China (973 Program) under Grant No. 2013CB632900. D. Y. Wang would like to thank for the support of the Australian Research Council Discovery Project (Grant No. DP110104629). This work was supported by the GRF Grant No. 514512 and the PolyU internal Grant No. G-YJ169.

[1]M. Liu, J. Liu, C. Ma, G. Collins, C. Chen, A. D. Alemayehu, G. Subramanyam, J. He, J. Jiang, E. I. Meletis, and A. Bhalla, CrystEngComm **15**, 6641 (2013).
[2]A. K. Tagantsev, V. O. Sherman, K. F. Astafiev, J. Venkatesh, and N. Setter, J. Electroceram. **11**, 5 (2003).
[3]W. F. Qin, J. Xiong, J. Zhu, J. L. Tang, W. J. Jie, Y. Zhang, and Y. R. Li, J. Mater. Sci. **43**, 409 (2008).
[4]B. Jaffe, W. R. Cook, and H. Jaffe, *Piezoelectric Ceramics* (Academic Press, New York and London, 1971).
[5]M. Kumar, A. Garg, R. Kumar, and M. C. Bhatnagar, Phys. B Condens. Matter **403**, 1819 (2008).
[6]J. Xu, W. Menesklou, and E. Ivers-Tiffée, J. Eur. Ceram. Soc. **25**, 2289 (2005).
[7]J. Y. Ha, C. Y. Kang, J. W. Choi, S. H. Sim, S. F. Karmanenko, S. J. Yoon, and H. J. Kim, Integr. Ferroelectr. **86**, 85 (2006).
[8]S. Sen and R. N. P. Choudhary, Mater. Chem. Phys. **87**, 256 (2004).
[9]H. Chen, C. Yang, C. Fu, J. Shi, J. Zhang, and W. Leng, J. Mater. Sci. Mater. Electron. **19**, 379 (2008).
[10]J. W. Xiong, B. Zeng, and W. Q. Cao, J. Electroceram. **21**, 124 (2008).
[11]J. Bera and S. K. Rout, J. Electroceram. **18**, 33 (2007).
[12]W. C. Xu, K. H. Lam, S. H. Choy, and H. L. W. Chan, Integr. Ferroelectr. **89**, 87 (2007).
[13]N. Y. Chan, G. Y. Gao, Y. Wang, and H. L. W. Chan, Thin Solid Films **518**, e82 (2010).
[14]Z. Yu, R. Guo, and A. S. Bhalla, Mater. Lett. **57**, 349 (2002).
[15]X. G. Tang, K. H. Chew, and H. L. W. Chan, Acta Mater. **52**, 5177 (2004).
[16]B. C. Luo, D. Y. Wang, M. M. Duan, and S. Li, Appl. Phys. Lett. **103**, 122903 (2013).
[17]W. Liu and X. Ren, Phys. Rev. Lett. **103**, 257602 (2009).
[18]J. Hao, W. Bai, W. Li, and J. Zhai, J. Am. Ceram. Soc. **95**, 1998 (2012).
[19]I. Coondoo, N. Panwar, H. Amorín, M. Alguero, and A. L. Kholkin, J. Appl. Phys. **113**, 214107 (2013).
[20]B. C. Luo, D. Y. Wang, M. M. Duan, and S. Li, Appl. Surf. Sci. **270**, 377 (2013).
[21]N. Y. Chan, Y. Wang, and H. L. W. Chan, Ferroelectrics **419**, 33 (2011).
[22]S. S. Gevorgian, T. Martinsson, P. L. J. Linnkr, S. Member, and E. L. Kollberg, IEEE Trans. Microwave Theor. Tech. **44**, 896 (1996).
[23]Y. Wang, N. Chong, Y. L. Cheng, H. L. W. Chan, and C. L. Choy, Microelectron. Eng. **66**, 880 (2003).
[24]N. Y. Chan, S. H. Choy, D. Y. Wang, Y. Wang, J. Y. Dai, and H. L. W. Chan, J. Mater. Sci. Mater. Electron. **25**, 2589 (2014).
[25]C. L. Canedy, H. Li, S. P. Alpay, L. Salamanca-Riba, A. L. Roytburd, and R. Ramesh, Appl. Phys. Lett. **77**, 1695 (2000).
[26]J. H. Chen, C. L. Lia, K. Urban, and C. L. Chen, Appl. Phys. Lett. **81**, 1291 (2002).
[27]N. Navi, H. Kim, J. S. Horwitz, H. D. Wu, and S. B. Qadri, Appl. Phys. A Mater. Sci. Process. **76**, 841 (2003).
[28]K. R. Udayakumar, P. J. Schuele, J. Chen, S. B. Krupanidhi, and L. E. Cross, J. Appl. Phys. **77**, 3981 (1995).
[29]Y. Lin, X. Chen, S. W. Liu, C. L. Chen, J.-S. Lee, Y. Li, Q. X. Jia, and A. Bhalla, Appl. Phys. Lett. **86**, 142902 (2005).
[30]D. Y. Wang, Y. Wang, X. Y. Zhou, H. L. W. Chan, and C. L.Choy, Appl. Phys. Lett. **86**, 212904 (2005).
[31]K. J. Choi, M. Biegalski, Y. L. Li, A. Sharan, J. Schubert, R. Uecker, P. Reiche, Y. B. Chen, X. Q. Pan, V. Gopalan, L.-Q. Chen, D. G. Schlom, and C. B. Eom, Science **306**, 1005 (2004).
[32]J. H. Haeni, P. Irvin, W. Chang, R. Uecker, P. Reiche, Y. L. Li, S. Choudhury, W. Tian, M. E. Hawley, B. Craigo, A. K. Tagantsev, X. Q. Pan, S. K. Streiffer, L. Q. Chen, S. W. Kirchoefer, J. Levy, and D. G. Schlom, Nature **430**, 758 (2004).
[33]L. L. Jiang, X. G. Tang, Y. P. Jiang, Q. X. Liu, C. B. Ma, and H. L. W. Chan, Surf. Coat. Technol. **229**, 162 (2013).
[34]J. Zhai, X. Yao, and H. Chen, Ceram. Int. **30**, 1237 (2004).
[35]X. G. Tang, J. Wang, and H. L. W. Chan, J. Cryst. Growth **276**, 453 (2005).